CHEMICAL ENGINEERING TRANSACTIONS
VOL. 73, 2019
A publication of AIDIC
The Italian Association of Chemical Engineering
Online at www.aidic.it/cet
Guest Editors: Andrea D'Anna, Paolo Ciambelli, Carmelo Sunseri

ISBN 978-88-95608-70-9; **ISSN** 2283-9216
DOI: 10.3303/CET1973045

Prospects of 2d Materials-Based Membranes in Water Desalination

Annarosa Gugliuzza[a]*, Francesca Macedonio[a], Antonio Politano[b], Enrico Drioli[a]

[a]Research Institute on Membrane Technology-National Research Council (CNR-ITM), Via Pietro Bucci 17C, Rende (CS) 87036, Italy
[b]Department of Physical and Chemical Sciences, University of L'Aquila, via Vetoio, 67100 L'Aquila, AQ, Italy
a.gugliuzza@itm.cnr.it

This study discloses the role of graphene and bismuth chalcogenides in membranes designed to water desalination. Nanocomposite membranes were tailored and characterized from morphological and physicochemical point of views. Membrane distillation (MD) and membrane crystallization (MCr) experiments were implemented in order to evaluate how confined fillers can affect the final performance of membrane process in terms of flux, rejection, nucleation and growth rate of salts crystals. Chemisorption was envisaged as a crucial mechanism in assisting water diffusion and ion aggregation.
This study provides new insightful indication about the powerful function of graphene and materials beyond graphene in membranes designed for scalable MD and MCr. Higher performances could make these membrane operations extremely challenging for future competitive water desalination processes.

1. Introduction

Water desalination is envisioned to be a rapid and effective solution to solve troubles related to fresh and drinkable water supply (Perrotta et al., 2017; Giurco et al., 2014). Membrane technology provides various tools for accomplishing this target (Drioli et a., 2017). Despite membrane reverse osmosis (RO) is one of the most popular membrane operation for water desalination, MD and MCr are regarded as two new generation and more promising processes to get fresh water and salt crystals from seawater (Etoumi and Jobson, 2018; Chabanon et al., 2016; Kiss et al., 2018). Both the processes take indeed numerous advantages over others, because they work at much lower pressure and temperature enabling one to regain fresh water and minerals with higher recovery factor. Independently of the configuration, this kind of technology uses basically hydrophobic microporous membranes to separate two phases (Gugliuzza and Basile, 2013). A liquid-vapour interface is established at the entrance of each single pore preventing mixing of two streams. The objective is to let water pass from liquid to vapour state under a driving force such as a difference of temperature (thermally driven operation) or solute concentration (osmotic operation). Water vapour is, hence, diffused through the pores of the membrane and condensed again at the permeate side, while the salts are retained.
However, the success of this process on scale is strongly dependent on high productivity-efficiency trade-off, which is not accomplished fully when commercial or traditional tailor-made membranes are worked. As far as structural features of the membrane are concerned, the use of new materials is strongly necessary to achieve a larger mass transfer together with a directed selectivity. This would imply a better quantity-quality ratio for fresh and reusable water and highest-quality crystals (Gugliuzza et al., 2011). There is a strong need to engineer membranes, which can become new interface paradigms for new concept fruitful membrane separation processes (Gugliuzza et al., 2017).
Dirac materials as graphene and topological insulators (especially, bismuth chalcogenides) have attracted considerable interest for applications in optoelectronics (Song et al., 2018; Zhang et al., 2009; Kathun et al., 2018). The use of this class of materials in other technological fields could be of extreme interest for the fabrication of new hybrid-composite membranes dedicated to the treatment of seawater (Macedonio et al., 2018; Gugliuzza et al., 2019). Herein, an overview is given on the attractive potential of graphene and

Paper Received: 23 April 2018; Revised: 27 August 2018; Accepted: 22 November 2018

Please cite this article as: Gugliuzza A., Macedonio F., Politano A., Drioli E., 2019, Prospects of 2D Materials-based Membranes in Water Desalination , Chemical Engineering Transactions, 73, 265-270 DOI:10.3303/CET1973045

materials beyond graphene in yielding better productivity-efficiency trade-off for advanced membrane separation processes such as MD and MCr.

2. Experimental section

2.1.Materials

PVDF (Solef®6020, Solvay Solexis: water adsorption <0.040% @23 °C after 24h; dp=1.78 Kg/m^3) was kindly supplied by Solavy Solexis. Commercial graphene platelets (GPs) powder and Bi_2Se_3 (Sigma Aldrich) were used as fillers. The polymer was dissolved in 1-Methyl-2-pyrrolidinone (NMP, Riedel de Haën: max 0.05% in water, d=1.03 Kg/m^3), whereas propan-2-olo (IPA, WWR PROLABO: d=0.78 Kg/m^3) was used as non-solvent.

2.2 Membrane Preparation

The membranes were prepared by dry-wet phase inversion. GPs and Bi_2Se_3 were dispersed in NMP using an ultrasonic bath alternated with mechanical stirring for 2 h at 30 °C. PVDF was, then, added to the mixture at a concentration of 12 wt.% and the mixtures were left under mechanical stirring at 30°C for 24 h, changing the GPs loading from 0.5 to 10 %, whereas for Bi_2Se_3 the content was 20 %. After degassing, the dopes were uniformly cast on glass plates by using a casting knife regulated on 250 μm (Elcometer Instruments Inc). The casting solutions were coagulated and left for 10 min in a bath containing IPA in order to promote solid-liquid demixing and then washed in ultra-pure water for more times. The films were, hence, air-dried at room temperature overnight and, finally, annealed at 30 °C for 1 h.

2.3 Characterization

Membrane morphology was examined by using SEM (Zeiss EVO MA10, Germany). Pore size and distribution were estimated according to the gas-liquid displacement technique (PM, Instruments). Samples with an effective area of 3.5 cm^2 were filled by FCO (3M) and the liquid was displaced from bigger to smaller pores with increasing pressure. The overall porosity was measured by filling them with FCO. The membrane weight was estimated before and after filling and the porosity was expressed in percentage as ratio between the volume occupied by the fluorinert liquid and the volume of the membrane. Six specimens were tested for each kind of nanocomposite membrane. The resistance to wetting from salt solutions was investigated by measuring the contact angle value with time according to sessile drop method (Cam 200 KSV instruments, LTD). X-ray photoelectron spectroscopy experiments were performed at Elettra synchrotron, Trieste, Italy, with photon energies in the 400-654 eV range. Water exposure was carried out at room temperature through leak valves.

2.4 MD and MCr tests

Thermally-driven MD and MCr experiments were executed accordingly with the Membrane Direct Contact (DC) configuration using NaCl solutions 0.6 M for MD – flow rate at feed side = 100 mL min^{-1}; flow rate at permeate side = 83 mL min^{-1}; T_{feed}= 38 to 56 ± 2 °C and T_{perm}= 15 °C. MCr experiments were implemented by using NaCl solutions 5.3 M – flow rate at feed side = 250 mL min^{-1}; flow rate at permeate side = 100 mL min^{-1}; T_{feed}= 35 ± 2 °C. In both the cases, retentate and distillate streams were converged, in a counter-current way, toward the membrane module containing the membrane, where the liquid water was evaporated. On the retentate side, a pump was taking and sending the heated feed to the membrane module. Also on the distillate side, a second pump ensured the counter-current recycle of the cold stream in order to remove from the solution the vapour diffusing through the membrane pores. The trans-membrane fluxes were estimated by evaluating the weight variations in the distillate tanks, whereas crystals recovery was performed from salt solutions in order to assess crystals nucleation and growth. The salt conductibility of the feed and permeate streams were measured by using a conductive meter (Eutech Instruments PC 2700). Sodium chloride crystals produced were observed by using an optic microscope (NIIKON, ECLIPSE LV100ND) and pictures recorded with a digital video-camera module DS-Fi2 equipped with optical head (10/100X).
Crystals were characterized according to different parameters, including crystals shape, dimension and growth rate. The evolution of particle size distribution as a function of time allowed the evaluation of the quality and the mean diameter of the produced crystals. Moreover, it was also possible to estimate the coefficients of variation (*CV*) and the growth rate of the produced crystals (*G*) according to the following equations:

$$\mathrm{CV} = \frac{\mathrm{F_{80\%} - F_{20\%}}}{2 \cdot \mathrm{F_{50\%}}} \cdot 100 \quad (1)$$

$$\ln(\mathrm{n}) = \frac{-\mathrm{L}}{\mathrm{Gt}} + \ln(\mathrm{n^0}) \quad (2)$$

$$B^0 = n^0 G \quad (3)$$

Where *F* is the cumulative percent function given by the crystal length at the indicated percentage, n is the crystal population density, *L* is crystal size, *G* is growth rate, t is retention time and n^0 is population density at *L* equal to zero (Cui et al., 2018).

3. Results and Discussion

Nanocomposite membranes were prepared by mixing graphene platelets (GP) and bismuth selenide (Bi_2Se_3) with polyvinylidinedifluoride (PVDF) according to dry-wet phase inversion. Microporous membranes with pore size ranging from 0.2 to 0.5 μm and overall porosity higher than 60% were tailored. BSE and SEM micrographs show typical spherulitic structures of PVDF entrapping Bi_2Se_3 and graphene, respectively (Figure 1).

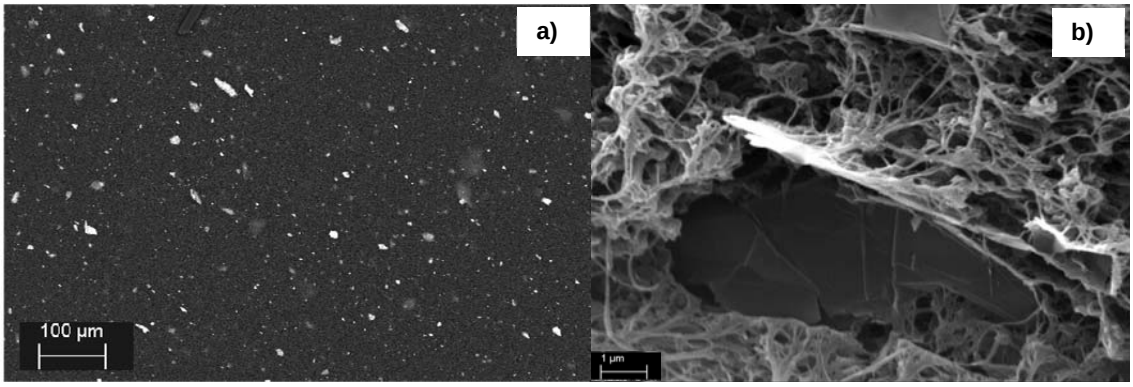

*Figure 1. BSE (**a**) and SEM (**b**) micrographs collected on the top surface of PVDF membranes entrapping Bi_2Se_3 (a) and graphene platelets (b), respectively.*

This kind of morphology provides a large resistance to wetting events, thus resulting in contact angle values of 130 ° for membranes containing Bi_2Se_3 20% and of around 150 ° for membranes containing GP at various loading (Figure 2). Such anti-wetting properties well match with one of the most important requirements of the membrane contactor technology dedicated to water desalination. Indeed, these membranes were tailored on order to explore their proficiency in water desalination processes such as MD and MCr, wherein membrane enables water diffusion as vapour whereas liquids are prevented from entering inside the pores.

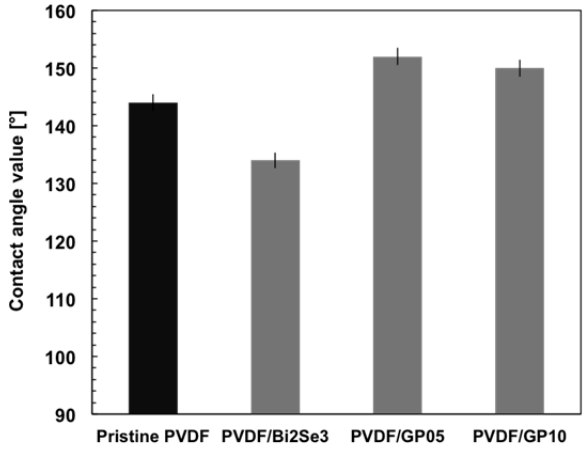

Figure 2. Contact-angle measurements carried out according to the sessile drop method on the top surface of nanocomposite PVDF membranes with solutions of NaCl at 0.6M

Remarkably, the focus of this work was to study the effects of the filler confined in polymeric matrix on flux, salt rejection as well as crystal nucleation and growth rate. With this purpose, MD and MCr experiments were implemented and the performances of composite membranes were compared under identical working conditions (Figure 3).

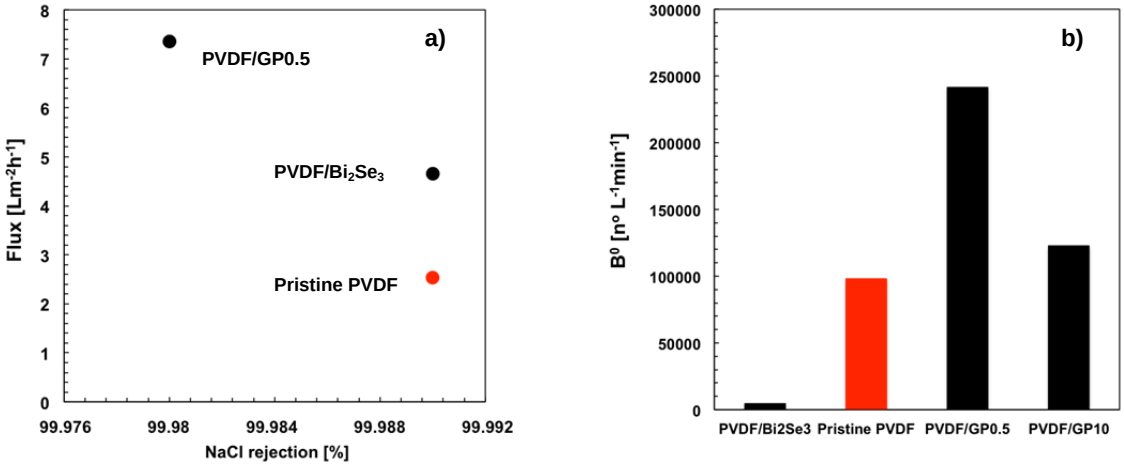

Figure 3. Flux-rejection trade-off estimated for composite PVDF membranes in MD operations (T_{feed}= 38 °C) (a); nucleation of crystals observed for PVDF composite membranes worked on MCr plants (T_{feed} = 35 °C) (b).

Figure 3a shows an increase in water flux when the filler is confined into polymer matrix. Much higher shift of the flux was estimated for PVDF membranes entrapping graphene platelets at 0.5%. In all cases, very high salt rejection values were achieved. Figure 3b shows the change in the crystal nuclei formation as a function of the filler confined in PVDF membranes.

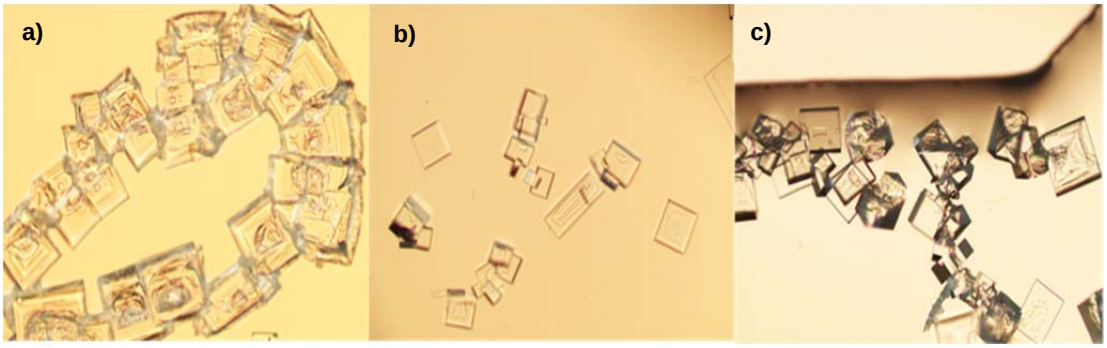

Figure 4. Pictures (@10X) of NaCl crystals after 8.3 h: a) PVDF/Bi_2Se_3; b) pristine PVDF; c) PVDF/GP10

As detected, Bi_2Se_3 yields a lower number of nuclei, which grow yet more quickly and uniformly when compared to pristine PVDF, leading to a CV value of 36 % against 55-63% estimated for other membranes. When the filler is graphene, much more massive nucleation of crystals is observed with a lower growth rate (Figure 4). The obtained crystals showed the characteristic cubic block-like form in accordance with the expected geometry of the NaCl crystals, though a small percentage of crystals exhibiting an elongated shape was observed in each sample.

As a result, the inclusion of fillers inside the membrane has an extraordinary capacity to enhance the removal of water molecules from ion–water clusters. The final result is the occurrence of ion-ion aggregation with remarked effects on the nucleation step, but also on the evolution of the crystals growth and size distribution.

The capability of the filler to uptake water is confirmed by XPS measurements carried out on surfaces of graphene, epitaxially grown on Ni(111) and Bi_2Se_3 single crystal (exfoliated in situ by micromechanical cleavage) exposed to water at room temperature (Figure 5). For graphene on Ni(111), both C-1s and O-1s core levels (Figure 5, top and middle panels) suggest the occurrence of water permeation under graphene cover, with a partial dissociation of water molecules, evidenced by the two components in the O-1s. The main

component (approximatively 80% of the total area of O-1s) is associated by molecular water, while the remaining 20% to hydroxyl groups. Thus, water splitting occurs, likely at graphene defects. Water fragments are totally desorbed at 750 K. The hydro-dehydrogenation process is fully reversible, as indicated by the analysis of the C-1s line-shape totally matching that of the pristine graphene after heating. Conversely, for H_2O/Bi_2Se_3 the small signal in O-1s is due to water adsorption at Se vacancies. In both cases in Fig. 5, water reactivity is driven by defects (Figure 5). Therefore, both epitaxial graphene and Bi_2Se_3 topological insulators are able to stabilize water at room temperature with partial dissociation for the case of graphene, with the subsequent formation of C-H groups. Water-induced graphene hydrogenation at room temperature enables novel pathways for energy storage and production (Politano, 2016). Specifically, based on experimental evidence, chemisorption mechanisms are hence suggested to promote water sequestration from salt solutions, thereby resulting in a more controlled formation and growth of crystals (Figure 4).

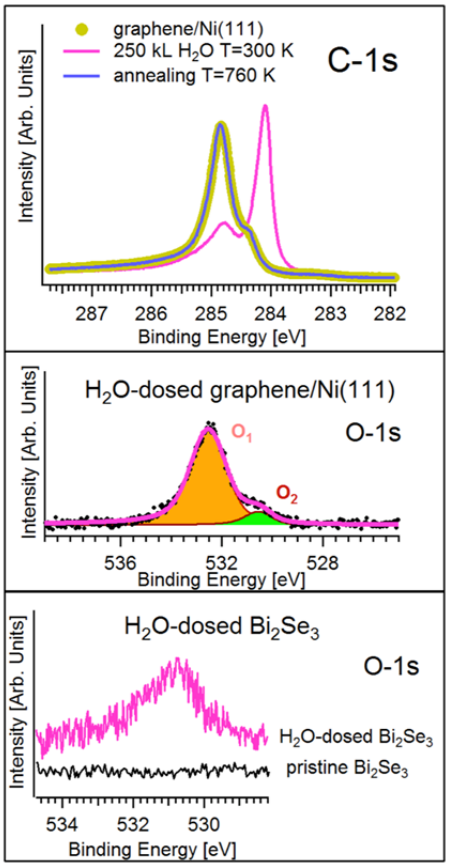

Figure 5. (Top panel) C-1s core level for graphene/Ni(111) surface and its modification upon dosage of 250 kL (1 L=10^{-6} torr·s) at room temperature and the successive heating at T=750 K. Photon energy is 400 eV (data from Politano, 2016). (Middle panel) O-1s core level for water-dosed graphene/Ni(111). Photon energy is 650 eV. The two components in the spectrum are associated to intact water molecules (denoted as "O_1") and hydroxyl group coming from water decomposition (denoted as "O_2"). Photon energy is 650 eV. Data have been taken from Politano, 2016. (Bottom panel) O-1s core level in pristine and H_2O-dosed (1000 L) Bi_2Se_3. Photon energy is 654 eV. Experiments and water dosage were carried out at room temperature. A Shirley background was subtracted from raw data. Data have been taken from Politano, 2014.

4. Conclusions

Graphene and bismuth selenide have been used to engineer nanocomposite membranes. These membranes have been tested in MD and MCr plants in order to assess the potential of new class of materials in water desalination. As a proof-of-concept, the flux was increased up to 200% with values of salt rejections approaching 100%. Accordingly, remarkable effects were also observed on nucleation, growth and uniformity of the crystals. By means of surface-science tools, it was also evidenced that reactivity toward water is associated to carbon vacancies in graphene (where water can also decompose) and Se vacancies in Bi_2Se_3.

Definitely, chemisorption mechanisms were envisaged to assist mass transfer, nucleation induction and growth rate, resulting in a quicker and better-quality formation of minerals. These preliminary results open new horizons towards the design of membranes based on innovative materials for the development of fruitful supply of fresh water and minerals.

Acknowledgments

This research has been funded by 'a grant from the Italian Ministry of Foreign Affairs and International Cooperation' within the frame of the Great Relevance International Project Italy (MAECI)-China (NSFC) 2018–2020 - New Materials, with particular reference to Two-dimensional systems and Graphene (Prot.MAE0065611). AP thanks Elettra synchrotron for the access to XPS facilities.

References

Chabanon E., Mngin D., Charcosset C., Membranes and crystallization processes: State of the art and prospects, 2016, J. Membr. Sci., 509, 57-67.

Cui Z., X Li, Y Zhang, Z Wang, A Gugliuzza, F Militano, E Drioli, F. Macedonio, 2018, Testing of three different PVDF membranes in membrane assisted-crystallization process: Influence of membrane structural-properties on process performance, Desalination, 440, 68-77

Drioli E., Ali A., Macedonio F., 2017, Membrane Operations for Process Intensification in Desalination, Appl. Sci., 7, 100

Etoumi A.E., Jobson M., 2018, Operational Optimization for Hybrid Membrane-Distillation Systems, 70, 457-462.

Giurco D.P., Turner A., Fane S., White S. B., 2014, Desalination for Urban Water: Changing Perceptions and Future Scenarios in Australia, Chemical Engineering Transactions, 42, 13-18.

Gugliuzza A., Aceto M.C., Drioli E., 2011, Interactive functional poly (vinylidene fluoride) membranes with modulated lysozyme affinity: a promising class of new interfaces for contactor crystallizers, Polym. Inter. 58, 1452-1464.

Gugliuzza A., Basile A., Membrane contactors: Fundamentals, membrane materials and key operations, 2013, Chapter in: A Basile (Ed.), Handbook of Membrane Reactors, Vol 2, Woodhead Publishing Limited, Cambridge, UK, 54-106.

Gugliuzza A., Politano A., Drioli E., 2019, Chapter in: E Drioli, L Giorno and A Gugliuzza (Eds.), Functional Nanostructured Membranes, Pan Stanford Publishing Pte. Ltd., Singapore, 193-223.

Gugliuzza A., Politano A., Drioli E., 2017, The advent of graphene and other two-dimensional materials in membrane science and technology, Curr. Opin. Chem. Eng. 16, 78-85.

Kiss A.A., Kattan Readi O.M., 2018, An industrial perspective on membrane distillation process, J. Chem. Technol. Biotechnol, 93, 2047-2055.

Khatun S., Bhunia H., Pal A.J., 2018, Bi_2Se_3 topological insulator at the 2D-limit: role of halide-doping on Dirac point, Phys. Chem. Chem. Phys., 20, 17934-17941.

Li W., Van der Bruggen B., Luis P., 2014, Integration of reverse osmosis and membrane crystallization for sodium sulphate recovery, Chemical Engineering and Processing: Process Intensification, 85, 57-68.

Macedonio F., Politano A., Drioli E., Gugliuzza A., 2018, Bi_2Se_3-assisted membrane crystallization, Mater. Horiz., 5, 912-919.

Politano A., Caputo M., Nappini S., Bondino F., Magnano E., Aliev Z.S., Babanly M.B.., Goldoni A., Chiarello G., Chulkov E. V., 2014, Exploring the Surface Chemical Reactivity of Single Crystals of Binary and Ternary Bismuth Chalcogenides, J. Phys. Chem. C 118, 21517–21522.

Politano A., Cattelan M., Boukhvalov D.W., Campi D., Cupolillo A., Agnoli S., Apostol N.G., Lacovig P., Lizzit S., Farias D., Chiarello G., Granozzi G., Larciprete R., 2016, Unveiling the Mechanisms Leading to H_2 Production Promoted by Water Decomposition on Epitaxial Graphene at Room Temperature, ACS Nano, 10, 4543-4549.

Song K., Soriano D., Cummings A.W., Robles R., Ordejón P., Roche S., 2018, Spin Proximity Effects in Graphene/Topological Insulator Heterostructures, Nano Lett., 18, 2033-2039.

Zhang H., Liu C-X., Qi X-L., Dai X., Fang Z., Zhang S-C., 2009, Topological insulators in Bi_2Se_3, Bi_2Te_3 and Sb_2Te_3 with a single Dirac cone on the surface, Nature Physics, 5, 438–442.